Cancer Science
The official journal of the Japanese Cancer Association

Mature acinar cells are refractory to carcinoma development by targeted activation of Ras oncogene in adult rats

Hajime Tanaka,[1] Katsumi Fukamachi,[2] Mitsuru Futakuchi,[2] David B. Alexander,[2] Ne Long,[2] Shojiro Tamamushi,[4] Kohtaro Minami,[5] Susumu Seino,[5] Hirotaka Ohara,[1] Takashi Joh[1] and Hiroyuki Tsuda[2,3,6]

[1]Departments of Gastroenterology and Metabolism, [2]Molecular Toxicology and [3]Nanotoxicology Project, Nagoya City University Graduate School of Medical Sciences, Nagoya; [4]CLEA Japan Inc., Shizuoka; [5]Division of Cellular and Molecular Medicine Kobe University Graduate School of Medicine, Kobe, Japan

(Received July 20, 2009/Revised October 8, 2009/Accepted October 13, 2009/Online publication November 16, 2009)

Pancreatic ductal adenocarcinoma (PDA) is one of the most debilitating malignancies in humans. A thorough understanding of the cytogenesis of this disease will aid in establishing successful treatments. We have developed an animal model which uses adult $Hras^{G12V}$ and $Kras^{G12V}$ transgenic rats in which oncogene expression is regulated by the Cre/loxP system and neoplastic lesions are induced by injection of adenovirus-expressing Cre recombinase. When adenovirus with Cre recombinase under the control of the CMV enhancer/chicken β-actin (CAG) promoter (Ad-CAG-Cre) is injected into the pancreatic duct of these animals, pancreatic neoplasias develop. Pathologically, the origin of these lesions is duct, intercalated duct, and centroacinar cells, but not acinar cells. The present study was undertaken to test the effect of acinar cell-specific oncogenic *ras* expression. Adult transgenic rats were injected with adenovirus with Cre recombinase under the control of the acinar cell-specific promoters amylase (Ad-Amy-Cre) and elastase-1 (Ad-Ela-Cre) or under the control of the non-specific CAG promoter. Injection of either Ad-Amy-Cre or Ad-Ela-Cre into the pancreatic ducts of transgenic animals in which oncogenic *Kras* is tagged with hemagglutinin (HA), HA-$Kras^{G12V}$ rats resulted in expression of oncogenic *ras* in acinar cells but not in duct, intercalated duct, or centroacinar cells. Notably, injected animals did not develop any observable proliferative or neoplastic lesions. In marked contrast, injection of Ad-CAG-Cre resulted in pancreatic cancer development within 4 weeks. These results indicate that adult acinar cells are refractory to Ras oncogene activation and do not develop neoplasia in this model. (*Cancer Sci* 2010; 101: 341–346)

Pancreatic ductal adenocarcinoma (PDA) is a highly lethal disease, which is usually diagnosed in an advanced state. Most patients die within 1 year of diagnosis, [1] and the 5-year survival rate is <5%.[2] Understanding of the cytogenesis of PDA offers new directions for targeted therapeutic approaches to combat this disease.

Previously, we reported on an animal model in which pancreatic neoplasia was induced in adult $Hras^{G12V}$ transgenic rats by injection of adenovirus with Cre recombinase under the control of the CMV enhancer/chicken β-actin (CAG) promoter into the pancreatic duct.[3] In these animals, it was shown that duct, intercalated duct, centroacinar, and acinar cells were all infected with the adenovirus, but induced pre-neoplastic and neoplastic lesions were shown to express only duct cell-specific characteristics and not acinar cell-specific characteristics. Moreover, proliferative lesions were not observed in acinar cells. Therefore, we hypothesized that PDA does not develop from adult pancreatic acinar cells in this model.

The present study was undertaken to directly test the capability of mature acinar cells to develop into a neoplastic lesion. Transgenic rats with an Hras or hemagglutinin (HA)-tagged Kras oncogene were injected with Cre recombinase expressing adenoviruses in which Cre expression was under the control of promoters specifically active in acinar cells. Mature acinar cells in injected rats did express active Ras proteins, but did not develop any proliferative or neoplastic lesions.

Materials and Methods

Generation of transgenic rats. For the generation of transgenic rats conditionally expressing human $Kras^{G12V}$, we first made a cDNA fragment encoding the human $Kras4B^{G12V}$ with a 3× HA tag sequence at its 5′ end (HA-$Kras^{G12V}$). The HA-$Kras^{G12V}$ cDNA was subcloned into the SacI/KpnI site of pCALNL5 (DNA Bank, RIKEN Bio Resource Center, Ibaraki, Japan)[4,5] to produce pCALNLHAKras. pCALNLHAKras was digested with SalI/HindIII. The purified cassette (Fig. 1A) was injected into the pronuclei of Sprague–Dawley rats (CLEA Japan, Tokyo, Japan). Techniques used for the generation of transgenic rats were the same as those reported previously.[3,6] A total of 265 injected eggs were transplanted into pseudo-pregnant Sprague–Dawley rats. Of 37 potential transgenic rats screened, four male and one female rat were shown by PCR to carry the transgene. Transgenic founder rats were mated with Sprague–Dawley rats, and offspring were screened for the presence of the transgene by PCR analysis of genomic DNA isolated from tail biopsies at the age of 3 weeks. The following primers were used: 5′-TCTGGATCAAATCCGAACGC-3′, 5′-TGACCTGCTGTGTC-GAGAAT-3′. Two founder rats carrying a CALNLHA$Kras^{G12V}$ transgene transmittable to descendent generations (Kras301and Kras327) and two founder rats (Kras409 and Kras417) carrying a non-tagged $Kras^{G12V}$ transgene were established using the same cassette (data not shown). In this study, we used Kras301 and Kras327. Hras250 rats conditionally expressing human $Hras^{G12V}$ were generated as previously described. [3] They were maintained in plastic cages in an air-conditioned room with a 12-h light/12-h dark cycle. All experiments were conducted according to the Guidelines for Animal Experiments of the Nagoya City University Graduate School of Medical Sciences.

Preparation of adenovirus vectors. Adenoviruses in which either the mouse amylase-2 or the rat elastase-1 promoter drove the expression of Cre recombinase (Ad-Amy-Cre or Ad-Ela-Cre) (Fig. 1B) were prepared as described previously.[7] Recombinant adenovirus vectors carrying the *Cre* gene (Ad-CAG-Cre) (Fig. 1B) and empty adenovirus vector were prepared as described previously.[3] Recombinant adenovirus vectors were amplified in HEK-293 cells and then purified using Vivapure

[6]To whom correspondence should be addressed.
E-mail: htsuda@med.nagoya-cu.ac.jp

doi: 10.1111/j.1349-7006.2009.01410.x

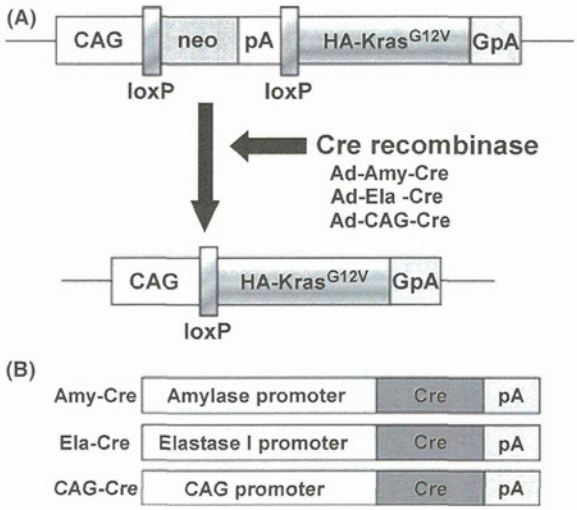

Fig. 1. Conditional expression of Kras^{G12V} transgene. (A) The CALNL-HAKras^{G12V} transgene is comprised of a hybrid CMV enhancer/chicken β-actin (CAG) promoter, a cassette for the neomycin resistance gene flanked by loxP sites, and a sequence containing a human Kras^{G12V} with a hemagglutinin (HA)-tag. Infection with the Cre recombinase-expressing adenovirus results in Cre-mediated recombination of the transgene and removal of the neo-coding region and its associated mRNA polyadenylation signal, generating a functional HA-Kras^{G12V} gene expression unit. GpA, rabbit- β-globin poly(A) site; pA, SV40 early poly(A) site. (B) Cre recombinase with nuclear localization signal expressing adenovirus in which Cre expression is under the control of three different promoters: the amylase promoter and the elastase-1 promoter which are active in acinar cells, and the CAG promoter which is a nonspecific promoter.

Adenopack (Vivascience, Hannover, Germany). The titer of the adenovirus was determined by using the Rapid titer kit (Clontech, Mountain View, CA, USA). The virus stock was concentrated to 1.0×10^{10} pfu/mL.

Induction of active Ras in the pancreas. Adenovirus vectors were injected into the pancreatic ducts of 12-week-old adult male rats through the common duct as previously reported. To induce active Ras specifically in acinar cells, adenoviruses (6×10^8 pfu/rat) in which the expression of Cre recombinase was under the control of acinar cell specific promoters, either the amylase-2 (Ad-Amy-Cre) or elastase-1 (Ad-Ela-Cre) promoter, were used. To induce active Ras non-specifically, adenoviruses (6×10^8 pfu/rat) in which the expression of Cre recombinase was under the control of the non-specific CAG promoter were used.

Western blotting. Western blot analysis and detection of activated Ras protein was performed using a Ras Activation Assay kit (Upstate, Lake Placid, NY, USA) as described previously.[3,8] Concentrations of the proteins were determined by Bio-Rad Protein assay. Proteins were separated by SDS-PAGE. After transfer to a polyviniliden defluoride membrane, the membrane was blocked with 5% nonfat milk and then incubated for 1 h at room temperature with primary antibodies. The following antibodies were used: anti-Ras, clone Ras10 (Upstate) diluted 1:4000; HA-probe (Y-11; Santa Cruz Biotechnology, Santa Cruz, CA, USA) diluted 1:1,000; and monoclonal anti-β-actin (A5441; Sigma, St Louis, MO) diluted 1:10 000. The primary antibodies were detected using HRP-conjugated secondary antibodies (Southern Biotechnology Associates, Birmingham, AL, USA) and ECL plus (GE Healthcare UK, Buckinghamshire, UK).

Immunostaining. Tissues were fixed in 10% formalin or 4% paraformaldehyde fixative and embedded in paraffin. For Ki67, proliferating cell nuclear antigen (PCNA), and HA-tag staining, sections were boiled for 10 min in a 10-mM citrate buffer (pH 6.0) and then allowed to cool in PBS for 30 min before incubation with antibodies. For anti-α-amylase staining, section slides were incubated for 10 min in a 0.1% trypsin solution at 37°C and then washed in PBS for 5 min before incubation with antibodies.

Before staining, each section was blocked with 10% goat serum (Nichirei Bio Science, Tokyo, Japan) for 5 min at room temperature. The slides were incubated overnight at 4°C with primary antibodies against Ki67antigen (NCL-Ki67-p; Novocastra Laboratories, Newcastle, UK), diluted 1:3000; PCNA (clone PC10; DakoCytomation, Glostrup, Denmark), diluted 1:50; HA-Tag (6E2; Cell Signaling, Danvers, MA, USA), diluted 1:100; or anti-α-amylase (A8273; Sigma, St Louis, MO, USA), diluted 1:200. Slides were incubated with secondary antibodies conjugated with Alexa Fluor488, 546, and 647 (Invitrogen, Carlsbad, CA, USA), and images were obtained with a FLUOVIEW FV300 confocal microscope (Olympus, Tokyo, Japan) or a BZ-9000 fluorescence microscope (Keyence, Osaka, Japan).

Results

Targeted activation of HA-Kras^{G12V} transgenes in mature acinar cells. Injection of transgenic rats with Cre recombinase expressing adenovirus resulted in excision of the stuffer DNA between the CAG promoter and the transgene and consequent expression of the transgene in infected cells (Fig. 1A). Kras301/ 327 rats were injected with Ad-Amy-Cre or Ad-Ela-Cre. Expression of HA-Kras^{G12V} was observed only in amylase-positive acinar cells and not in duct, centroacinar, intercalated duct, or islet cells (Table 2) (Fig. 2A; data for Ad-Ela-Cre is identical to that of Ad-Amy-Cre). Some acinar cells with nuclei with an ''owl-eye'' or ''ground glass'' appearance, which are generally used for identification of virus-infected cells,[9] in rats treated with Ad-Amy-Cre or Ela-Cre were also positive for both amylase and HA (Fig. 2A-d,e). All acinar cells positive for HA were entirely negative for Ki67 (Fig. 2A).

Lack of PDA development by targeted activation of Ras^{G12V} in mature acinar cells. None of the Kras301/327 rats injected with Ad-Amy-Cre or Ela-Cre developed pancreatic lesions (Ad-Amy-Cre, 0 out of 5; Ad-Ela-Cre, 0 out of 7) after 8 weeks (Fig. 2B, Table 1). Similarly, none of the Hras250 rats injected with Ad-Amy-Cre or Ad-Ela-Cre (6×10^8 pfu/rat) developed pancreatic lesions (Ad-Amy-Cre, 0 out of 7; Ad-Ela-Cre, 0 out of 8) after 8 weeks (Table 1). In addition, Kras301/327 rats injected with higher titers of Ad-Amy-Cre (6×10^9 pfu/rat) did not develop pancreatic lesions (data not shown). Finally, tumor induction was not observed in injected Kras301/327 rats even after 6 months (data not shown).

Neoplasia development by activation of Ras^{G12V} transgenes in ductular cells. Both Kras301/327 and Hras250 rats injected with Ad-CAG-Cre (6×10^8 pfu/rat) developed pancreatic neoplasias: 22 of 22 Kras301/327 rats and 30 of 35 and Hras250 rats after 2 to 4 weeks (Table 1), as observed in our previous report.[3] Pancreatic neoplasias were also observed in Kras301/327 rats injected with lower titers of Ad-CAG-Cre (6×10^7 pfu/rat) (data not shown). Activation of the transgene in the pancreatic ductal lesions of Kras301/327 rats was shown by Western blotting using anti-HA antibody (Fig. 3). The expression of HA-Kras^{G12V} was detected in pancreatic intraepithelial neoplasia (PanIN) and neoplastic lesions, but not in normal-looking pancreatic duct cells or stromal cells (Fig. 4A). Ki67 or PCNA and HA were positive in PanIN lesions (Fig. 4B) and in many neoplastic cells (Fig. 4C).

Discussion

The morphological and molecular signatures associated with human pancreas tumors suggests that duct epithelium is

doi: 10.1111/j.1349-7006.2009.01410.x

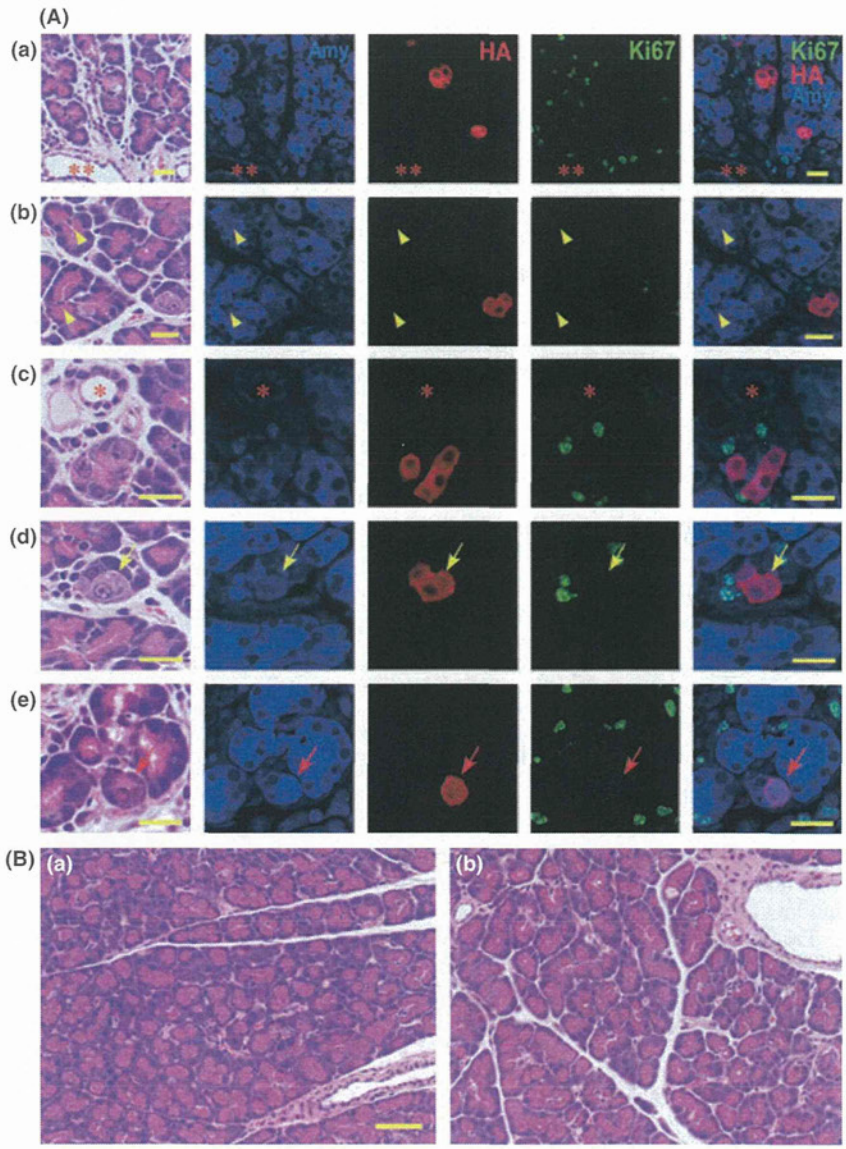

Fig. 2. Acinar cell-specific expression of hemagglutinin (HA)-Kras^{G12V}. (A) Localization of amylase (blue) protein, HA-Kras^{G12V} (red) and Ki67 (green) at 2 days after injection of virus with Ad-Amy-Cre (a, b, c, d) and Ela-Cre (e). All the HA-Kras^{G12V} positive cells (red) were acinar cells; expression was not observed in duct cells (**), centroacinar cells (yellow arrowhead), or small duct cells (*). Most virally infected acinar cells positive for HA-Kras^{G12V} were indistinguishable from non-infected acinar cells by hematoxylin–eosin staining. Some infected acinar cells have nuclei with a so-called "owl-eye" (yellow arrows) or "ground glass" (red arrows) appearance. Ki67 (green) is not present in the nuclei of the cells expressing HA-Kras^{G12V} (red). Bar, 20 μm. (B) None of the Ad-Amy-Cre (a) or the Ad-Ela-Cre (b) groups displayed any pancreatic lesions, even after 8 weeks. Bar, 50 μm.

responsible for the development of PDA, but it remains unclear whether other pancreatic cells might also contribute to the cytogenesis of these lesions. In our previous study using the Hras250 rat, 4 weeks after injection of adenovirus with Cre recombinase under the control of the constitutive CAG promoter, proliferative lesions in the duct epithelium, intercalated ducts, and centroacinar cells were widespread, but we could not detect any proliferative lesions in acinar cells; moreover, subsequent neoplastic lesions expressed only duct cell-specific characteristics and not acinar cell-specific ones.[3] We have obtained essentially identical results with Kras transgenic rats as we did with Hras250 rats (data not shown). These results suggest that PDAs may arise from centroacinar cells, intercalated duct, or pancreatic duct epithelium, but not from acinar cells.

The current study was undertaken to clarify whether mature acinar cells in adult rats could be induced to develop to PDA by targeted activation of oncogenic *ras*. Activation of oncogenic *ras* in acinar cells did not lead to the development of any observable pancreatic lesions, while nonspecific activation of oncogenic *ras* in the pancreas resulted in rapid development of

Table 1. Pancreas tumor induction by activation of Hras^{G12V} or hemagglutinin (HA)-Kras^{G12V} oncogene after Cre-adenovirus injection

Oncogene	Virus vector	Number of rats with tumor (%)
Hras^{G12V}	Amylase-Cre	0/7 (0)
	Elastase-Cre	0/8 (0)
	CAG-Cre	30/35 (87.5)
HA-Kras^{G12V}	Amylase-Cre	0/5 (0)
	Elastase-Cre	0/7 (0)
	CAG-Cre	22/22 (100)

Table 2. Target cell and tumor type in Hras^{G12V} and hemagglutinin (HA)-Kras^{G12V}transgenic rats

Virus vector	Target cells			Tumor yield	
	Acinar cells	Centroacinar cells	Duct cells	Acinar cells	Duct cells
Amy-Cre	+	–	–	–	–
Ela-Cre	+	–	–	–	–
CAG-Cre[3]	+	+	+	–	+

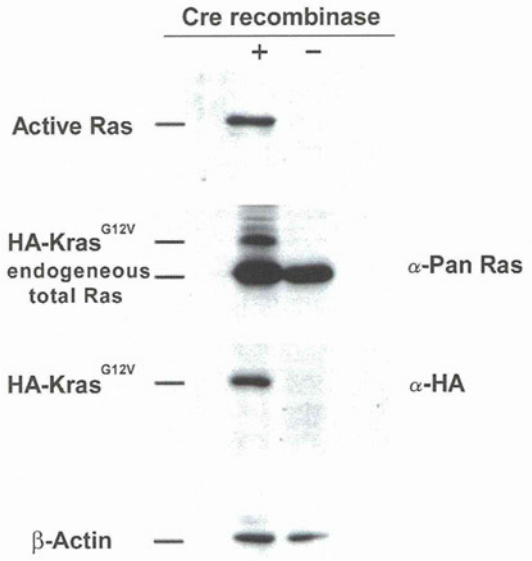

Fig. 3. Transgene activation in Kras301 and 327 by Western blotting. A high level of active Ras and hemagglutinin (HA)-Kras^{G12V} were detected in the pancreas of the Ad-CAG-Cre-treated rats. The amount of active Ras was analyzed by RBD (Ras-binding domain of Raf-1) pull-down assay followed by Western blotting with anti-pan Ras antibody. HA-Kras^{G12V} and endogeneous total Ras was detected using anti-Pan Ras antibody. HA-Kras^{G12V} was detected using anti-HA antibody. β-Actin was used as a loading control.

pancreatic neoplasias. Our results clearly show that conditional expression of oncogenic *ras* in acinar cells in fully developed pancreas tissue does not result in induction of neoplasia in this model (Table 1).

Previous reports in which Kras was activated in immature acinar cells during embryonic development[10,11] suggested that acinar-ductal metaplasia played a role in the development of PDA. In these models, premalignant acinar-ductal metaplasia and acinar tumor mixed with duct-like lesions developed in transgenic mice. This acinar-ductal metaplasia, however, may have occurred before the pancreas fully developed. Our model, on the other hand, targets mature acinar cells which express digestive enzymes, amylase and/or elastase, and these cells do not undergo acinar-ductal metaplasia in response to ras activation.

Our results are in agreement with a recent study in which the distribution of *K-RAS2* gene mutations was extensively examined in surgically resected pancreata from human patients and which concluded that ductal neoplasms of the human pancreas did not appear to arise from acinar cells.[12]

Kras mutations were not observed in pancreatic acinar cell carcinoma (ACC) induced in mature rats by administration of azaserine.[13] Furthermore, alterations in the APC/β-catenin pathway were detected in 23.5% of human ACC,[14] but mutation of Kras was not observed.[15,16] Thus, it is possible that APC/β-catenin or another pathway, but not necessarily Kras activation, is involved in ACC development.

While pancreas cancer in the hamster model is also believed to arise from ductal epithelial hyperplasia,[17,18] several studies using transgenic mice[11,19–24] suggest that PDA may develop from acinar cells. In most of these studies, however, oncogenic stimuli are present during embryonic development, prior to the development of a mature pancreas. Therefore, the acinar cells which were activated and developed into neoplasias in these models could very well be at a different developmental stage to the acinar cells which are present in a mature pancreas. This is important because the majority of PDA patients are 60 years of age or older. It is highly unlikely that an oncogenic insult occurring in the uterus is the root cause of most of these PDAs. Moreover, epidemiological studies indicate the incidence of PDA is closely related to lifestyle.[25] Therefore, PDA most likely develops from cells in the mature pancreas. Consequently, pancreas tumor models in which the oncogenic insult occurs during embryonic development are unlikely to be appropriate for determining the cytogenesis of human PDA.

Two models[22–24] use conditional activation of Cre recombinase to active oncogenic *ras* in adult animals: one model[22] uses the tet-off system to control expression of Cre recombinase and the other model[23,24] uses the tamoxifen-estrogen receptor system to control nuclear localization of Cre recombinase. These studies had slightly conflicting results. In one study, expression of oncogenic *ras* in adult acinar cells did not by itself induce pancreatic lesions; additional treatment causing chronic pancreatitis was also needed.[22] In the other study, expression of oncogenic *ras* was sufficient to induce PanIN-like lesions.[23,24] In our model, we clearly showed that while expression of oncogenic *ras* is sufficient to induce duct, intercalated duct, and/or centroacinar cells to develop into pancreatic cancers, it is not sufficient to induce acinar cells to develop into pancreatic cancers. Whether these discrepancies are due to experimental procedures, the nature of the Cre recombinase constructs used, or differences between mice and rats remains to be resolved. There are however, a few readily apparent differences. In our rat system, there is no expression of Cre recombinase in the animal until injection of adenovirus-expressing Cre recombinase, and the expression of Cre recombinase is transient. In the model which uses tamoxifen, on the other hand, Cre recombinase is expressed during embryonic development, but nuclear localization is regulated by tamoxifen.[23,24] In this model, however, there was a low level of tamoxifen-independent recombination events resulting in expression of oncogenic *ras* in embryonic acinar cells.[24] It is possible that embryonic acinar cells expressing oncogenic *ras* did not fully differentiate in the adult pancreas; for example, in the mouse colon expression of Kras^{G12V} inhibits differentiation.[26] Therefore, it is possible that in the tamoxifen-estrogen regulated model,[23,24] the acinar cells which were activated to undergo metaplasia to duct-like cells in the adult were not actually mature acinar cells. The other obvious difference is that in the model regulated by the tet-off system, two events were required to induce pancreas cancer: activation of oncogenic *Kras* and chronic pancreatitis.[22] Chronic pancreatitis would very likely result in the death of mature acinar cells and their replacement from a proliferative compartment. It is possible that these replacement cells are not fully mature acinar cells, again suggesting the possibility that the acinar cells which underwent metaplasia to duct-like cells were not actually mature acinar cells.

The primary aim of this study was to determine whether activation of oncogenic Kras in mature, digestive enzyme-secreting acinar cells would lead to pancreatic lesions. Our findings support our earlier hypothesis that PDA does not develop from Kras activation in mature acinar cells. It is possible, however, that PDA could develop from Kras activation in immature acinar cells, and in this regard we would like to emphasize the results of Guerra *et al.*[22] in which activation of Kras in the mature pancreas accompanied by chronic pancreatitis resulted in induction of PDA in transgenic mice. Importantly, chronic pancreatitis has been shown to be one of the main risk factors for PDA development in humans.[27,28]

Other factors which may influence PDA development in our model are inflammation and fibrosis. Shortly after infection of pancreatic tissue with Cre recombinase carrying adenovirus to activate the Kras transgene, infiltration of macrophages and lymphocytes could be observed. This infiltration is presumably in response to viral infection. A moderate degree of inflammation, however, was still observed in the stromal tissue surrounding the tumors when PDA developed. These finding suggest that

doi: 10.1111/j.1349-7006.2009.01410.x

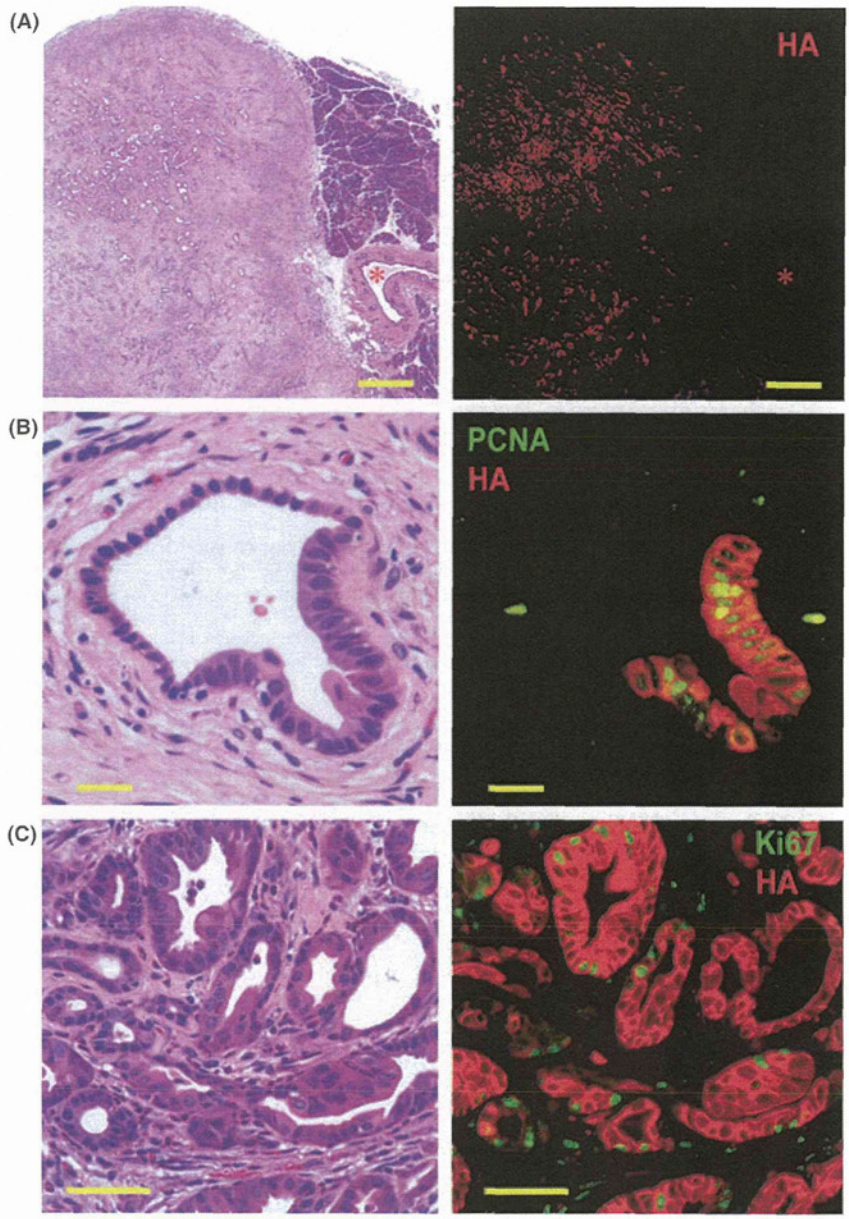

Fig. 4. Pancreatic ductal adenocarcinoma (PDA) induced by injection of Ad-CAG-Cre in Kras301/327 rats. (A) The expression of hemagglutinin (HA)-$Kras^{G12V}$ (red) was seen only in PDA lesions (on the left of photo), and not in stromal cells, acinar cells (on the right of photo), or normal pancreatic duct cells (*). Bar, 500 μm. (B) A pancreatic intraepithelial neoplasia (PanIN) lesion was surrounded by fibrous tissue with some infiltration of inflammatory cells. Expression of proliferating cell nuclear antigen (PCNA) (green) and HA protein (red) in a PanIN lesion in rats of the CAG-Cre group. PCNA is preferentially expressed in PanIN cells. Bar, 20 μm. (C) Expression of Ki67 (green) and HA protein (red) in PDA cells. Many PDA cells (red) are simultaneously positive for Ki67. Bar, 50 μm.

inflammation may play a role in PDA development in this model. However, interaction between the immune system and tumors is complex and whether inflammation actually promotes PDA development in this model remains to be examined.

A current study has demonstrated that the fibrous element accompanying inflammation can also play an important role in cancer development.[29] This aspect of PDA development in our model also remains to be examined.

In summary, while there are discrepancies between different animal models of pancreatic cancer, our results indicate that expression of oncogenic *ras* in fully mature acinar cells does not induce cell proliferation or result in development of any pancreatic lesions. Thus, we conclude that mature acinar cells are not the origin of PanIN or pancreatic neoplasia in this model.

Acknowledgments

We thank Dr T. Shirai (Nagoya City University) for his kind advice for histological examination and assistance in histological specimen preparation. This work was supported in part by a Grant-in-Aid for Scientific Research (C) from Japan Society for the Promotion of Science; a Grant-in-Aid for Cancer Research (15-2, 16-13, 17S-6, 20S-8) from the Ministry of Health, Labour and Welfare, Japan; a Grant-in-Aid for Research on Nanotechnical Medical (H19-Nano-Ippan-014) from the Ministry of Health, Labour, and Welfare of Japan; a Grant-in-Aid for Research on Risk of Chemical Substances (H19-Kagaku-Ippan-006) from the Ministry of Health, Labour, and Welfare of Japan; and a Grant-in-Aid for Nagoya Ohjinkai Young Investigators Medical Research Award from Nagoya City University, Japan.

References

1 Beger HG, Rau B, Gansauge F, Poch B, Link KH. Treatment of pancreatic cancer: challenge of the facts. *World J Surg* 2003; **27**: 1075–84.
2 Jemal A, Siegel R, Ward E, Murray T, Xu J, Thun MJ. Cancer statistics, 2007. *CA Cancer J Clin* 2007; **57**: 43–66.
3 Ueda S, Fukamachi K, Matsuoka Y *et al.* Ductal origin of pancreatic adenocarcinomas induced by conditional activation of a human Ha-ras oncogene in rat pancreas. *Carcinogenesis* 2006; **27**: 2497–510.
4 Kanegae Y, Lee G, Sato Y *et al.* Efficient gene activation in mammalian cells by using recombinant adenovirus expressing site-specific Cre recombinase. *Nucleic Acids Res* 1995; **23**: 3816–21.

5 Niwa H, Yamamura K, Miyazaki J. Efficient selection for high-expression transfectants with a novel eukaryotic vector. *Gene* 1991; **108**: 193–9.
6 Asamoto M, Ochiya T, Toriyama-Baba H *et al.* Transgenic rats carrying human c-Ha-ras proto-oncogenes are highly susceptible to N-methyl-N-nitrosourea mammary carcinogenesis. *Carcinogenesis* 2000; **21**: 243–9.
7 Minami K, Okuno M, Miyawaki K *et al.* Lineage tracing and characterization of insulin-secreting cells generated from adult pancreatic acinar cells. *Proc Natl Acad Sci U S A* 2005; **102**: 15116–21.
8 Fukamachi K, Imada T, Ohshima Y, Xu J, Tsuda H. Purple corn color suppresses Ras protein level and inhibits 7,12-dimethylbenz[a]anthracene-induced mammary carcinogenesis in the rat. *Cancer Sci* 2008; **99**: 1841–6.
9 Kobayashi TK, Sato S, Tsubota K, Takamura E. Cytological evaluation of adenoviral follicular conjunctivitis by cytobrush. *Ophthalmologica* 1991; **202**: 156–60.
10 Schmid RM. Acinar-to-ductal metaplasia in pancreatic cancer development. *J Clin Invest* 2002; **109**: 1403–4.
11 Grippo PJ, Nowlin PS, Demeure MJ, Longnecker DS, Sandgren EP. Preinvasive pancreatic neoplasia of ductal phenotype induced by acinar cell targeting of mutant Kras in transgenic mice. *Cancer Res* 2003; **63**: 2016–9.
12 Shi C, Hong SM, Lim P *et al.* KRAS2 mutations in human pancreatic acinar-ductal metaplastic lesions are limited to those with PanIN: implications for the human pancreatic cancer cell of origin. *Mol Cancer Res* 2009; **7**: 230–6.
13 Longnecker DS, Curphey TJ. Adenocarcinoma of the pancreas in azaserine-treated rats. *Cancer Res* 1975; **35**: 2249–58.
14 Abraham SC, Wu TT, Hruban RH *et al.* Genetic and immunohistochemical analysis of pancreatic acinar cell carcinoma: frequent allelic loss on chromosome 11p and alterations in the APC/beta-catenin pathway. *Am J Pathol* 2002; **160**: 953–62.
15 Terhune PG, Memoli VA, Longnecker DS. Evaluation of p53 mutation in pancreatic acinar cell carcinomas of humans and transgenic mice. *Pancreas* 1998; **16**: 6–12.
16 Van Kranen HJ, Vermeulen E, Schoren L *et al.* Activation of c-K-ras is frequent in pancreatic carcinomas of Syrian hamsters, but is absent in pancreatic tumors of rats. *Carcinogenesis* 1991; **12**: 1477–82.
17 Tsutsumi M, Kondoh S, Noguchi O *et al.* K-ras gene mutation in early ductal lesions induced in a rapid production model for pancreatic carcinomas in Syrian hamsters. *Jpn J Cancer Res* 1993; **84**: 1101–5.
18 Tsutsumi M, Konishi Y. Precancerous conditions for pancreatic cancer. *J Hepatobiliary Pancreat Surg* 2000; **7**: 575–9.
19 Tuveson DA, Zhu L, Gopinathan A *et al.* Mist1-KrasG12D knock-in mice develop mixed differentiation metastatic exocrine pancreatic carcinoma and hepatocellular carcinoma. *Cancer Res* 2006; **66**: 242–7.
20 Hingorani SR, Petricoin EF, Maitra A *et al.* Preinvasive and invasive ductal pancreatic cancer and its early detection in the mouse. *Cancer Cell* 2003; **4**: 437–50.
21 Wagner M, Luhrs H, Kloppel G, Adler G, Schmid RM. Malignant transformation of duct-like cells originating from acini in transforming growth factor transgenic mice. *Gastroenterology* 1998; **115**: 1254–62.
22 Guerra C, Schuhmacher AJ, Canamero M *et al.* Chronic pancreatitis is essential for induction of pancreatic ductal adenocarcinoma by K-Ras oncogenes in adult mice. *Cancer Cell* 2007; **11**: 291–302.
23 Habbe N, Shi G, Meguid RA *et al.* Spontaneous induction of murine pancreatic intraepithelial neoplasia (mPanIN) by acinar cell targeting of oncogenic Kras in adult mice. *Proc Natl Acad Sci U S A* 2008; **105**: 18913–8.
24 De La OJ, Emerson LL, Goodman JL *et al.* Notch and Kras reprogram pancreatic acinar cells to ductal intraepithelial neoplasia. *Proc Natl Acad Sci U S A* 2008; **105**: 18907–12.
25 Jiao L, Mitrou PN, Reedy J *et al.* A combined healthy lifestyle score and risk of pancreatic cancer in a large cohort study. *Arch Intern Med* 2009; **169**: 764–70.
26 Haigis KM, Kendall KR, Wang Y *et al.* Differential effects of oncogenic K-Ras and N-Ras on proliferation, differentiation and tumor progression in the colon. *Nat Genet* 2008; **40**: 600–8.
27 Lowenfels AB, Maisonneuve P, Cavallini G *et al.* Pancreatitis and the risk of pancreatic cancer. International Pancreatitis Study Group. *N Engl J Med* 1993; **328**: 1433–7.
28 Malka D, Hammel P, Maire F *et al.* Risk of pancreatic adenocarcinoma in chronic pancreatitis. *Gut* 2002; **51**: 849–52.
29 Sangai T, Ishii G, Kodama K *et al.* Effect of differences in cancer cells and tumor growth sites on recruiting bone marrow-derived endothelial cells and myofibroblasts in cancer-induced stroma. *Int J Cancer* 2005; **115**: 885–92.

doi: 10.1111/j.1349-7006.2009.01410.x

Induction of long interspersed nucleotide element-1 (L1) retrotransposition by 6-formylindolo[3,2-*b*] carbazole (FICZ), a tryptophan photoproduct

Noriyuki Okudaira[a,b], Kenta Iijima[a], Takayoshi Koyama[a], Yuzuru Minemoto[a], Shigeyuki Kano[a,b], Akio Mimori[a], and Yukihito Ishizaka[a,1]

[a]National Center for Global Health and Medicine, Shinjuku-ku, Tokyo 162-8655, Japan; and [b]Graduate School of Comprehensive Human Sciences, University of Tsukuba, Tsukuba 305-8577, Japan

Edited* by George R. Stark, Lerner Research Institute, Cleveland, OH, and approved August 24, 2010 (received for review February 5, 2010)

Long interspersed nucleotide element-1 (L1) is a retroelement comprising about 17% of the human genome, of which 80–100 copies are competent as mobile elements (retrotransposition: L1-RTP). Although the genetic structures modified during L1-RTP have been clarified, little is known about the cellular signaling cascades involved. Herein we found that 6-formylindolo[3,2-*b*]carbazole (FICZ), a tryptophan photoproduct postulated as a candidate physiological ligand of the aryl hydrocarbon receptor (AhR), induces L1-RTP. Notably, RNA-interference experiments combined with back-transfection of siRNA-resistant cDNAs revealed that the induction of L1-RTP by FICZ is dependent on AhR nuclear translocator-1 (ARNT1), a binding partner of AhR, and the activation of cAMP-responsive element-binding protein. However, our extensive analyses suggested that AhR is not required for L1-RTP. FICZ stimulated the interaction of the L1-encoded open reading frame-1 (ORF1) and ARNT1, and recruited ORF1 to chromatin in a manner dependent on the activation of mitogen-activated protein kinase. Along with our additional observations that the cellular cascades for FICZ-induced L1-RTP were different from those of L1-RTP triggered by DNA damage, we propose that the presence of the cellular machinery of ARNT1 mediates L1-RTP. A possible role of ARNT1-mediated L1-RTP in the adaptation of living organisms to environmental changes is discussed.

ARNT1 | ORF1 | cAMP-responsive element-binding protein | MAPK | chromatin recruitment

About 45% of the human genome is composed of transposable elements (1, 2). Long interspersed nucleotide element-1 (LINE-1; L1) is the most abundant component of retroelements, comprising about 17% of the human genome (1, 3). Its structural alignment is conserved from fish to human with two encoded proteins, open reading frames 1 and 2 (ORF1 and 2), the molecular weights of which are about 40 and 150 kDa, respectively (3, 4). ORF1 is a basic protein that binds mRNA, whereas ORF2 has dual functions of endonuclease and reverse-transcriptase activities (3). ORF1 and 2 can complete the retrotransposition of L1 (L1-RTP), which is processed by three steps: transcription, reverse transcription, and the insertion of newly synthesized L1-DNA into the host genome by target-primed reverse transcription (3). Among about 5×10^5 copies of human L1, 80–100 copies are competent as mobile elements (5), and genome shuffling by L1-RTP generates unique expression profiles depending on the integration sites of newly synthesized L1 DNA (6). DNA damage is a reported trigger of L1-RTP (7), but the cellular cascades involved or other factors responsible for the induction of L1-RTP are largely unknown.

The aryl hydrocarbon receptor (AhR), a basic helix–loop–helix/Per–Arnt–Sim (bHLH/PAS) transcription factor, is conserved in invertebrates to human (8, 9), and it recognizes various polycyclic aromatic hydrocarbons (10). For example, 2,3,7,8-tetrachlorodibenzo-*p*-dioxin (TCDD), a well-characterized AhR ligand, induces heterodimer formation (AhR complex; AHRC) of AhR and AhR nuclear translocator-1 (ARNT1). Depending on the nuclear localization signal (NLS) of ARNT1 (11), AHRC is translocated to the nucleus, recognizes the xenobiotic response element (XRE), and induces gene expression such as *CYP1A1* mRNA (12). Sequence similarities among species and physiological functions support the idea that AHRC was an innovation in vertebrates that enabled them to metabolize xenobiotics in their environments (8). However, its real function remains elusive due to a lack of definite information about its authentic ligands (8, 12).

As a candidate physiological AhR ligand, 6-formylindolo[3,2-*b*]carbazole (FICZ) is of particular interest. FICZ is generated from tryptophan by ultraviolet B irradiation (13, 14), and its metabolite has been identified in human urine (15). FICZ has a high affinity for AhR (13) and induces *CYP1A1* mRNA depending on the AhR (14, 16). Intriguingly, studies have proposed recently that FICZ and TCDD are differentially involved in T-cell differentiation: FICZ generates proinflammatory T cells (T_H17), whereas TCDD induces regulatory T cells (T_{reg}) (17, 18). These observations suggest that AhR ligands have novel, uncharacterized biological functions.

In the current study, we found that FICZ induced L1-RTP and that the induction of L1-RTP by FICZ depended on ARNT1, but not on AhR. Biochemical analysis revealed that FICZ activated mitogen-activated protein kinase (MAPK) and phosphorylated cAMP-responsive element-binding protein (CREB) (19), both of which were required for L1-RTP. Furthermore, FICZ induced the association of ORF1 and ARNT1, and recruited ORF1 to chromatin. These data suggest the presence of ARNT1-mediated genome shuffling by L1-RTP, and we discuss its possible involvement in the adaptation of living organisms to environmental changes.

Results

FICZ Induces L1-RTP. We first assessed FICZ-induced L1-RTP by a colony assay using pCEP4/L1*mneo*I/ColE1 (pL1-Neo^R) (20); its schematic representation is depicted in Fig. 1*A*. pL1-Neo^R contains all the components of the L1 gene and an inversely inserted transcriptional unit encoding a neomycin-resistant (Neo^R) gene as a reporter. The Neo^R gene had sequences of splicing donor (SD) and splicing acceptor (SA) in a sense orientation (*SI Methods*). The effects of FICZ on HuH-7 and HeLa cells were examined according to the experimental protocol (Fig. 1*A Lower*). As shown

Author contributions: N.O., S.K., A.M., and Y.I. designed research; N.O., T.K., and Y.I. performed research; N.O., K.I., T.K., and Y.M. contributed new reagents/analytic tools; N.O., T.K., and Y.I. analyzed data; and Y.I. wrote the paper.

The authors declare no conflict of interest.

Freely available online through the PNAS open access option.

*This Direct Submission article had a prearranged editor.

See Commentary on page 18239.

[1]To whom correspondence should be addressed. E-mail: zakay@ri.ncgm.go.jp.

This article contains supporting information online at www.pnas.org/lookup/suppl/doi:10.1073/pnas.1001252107/-/DCSupplemental.

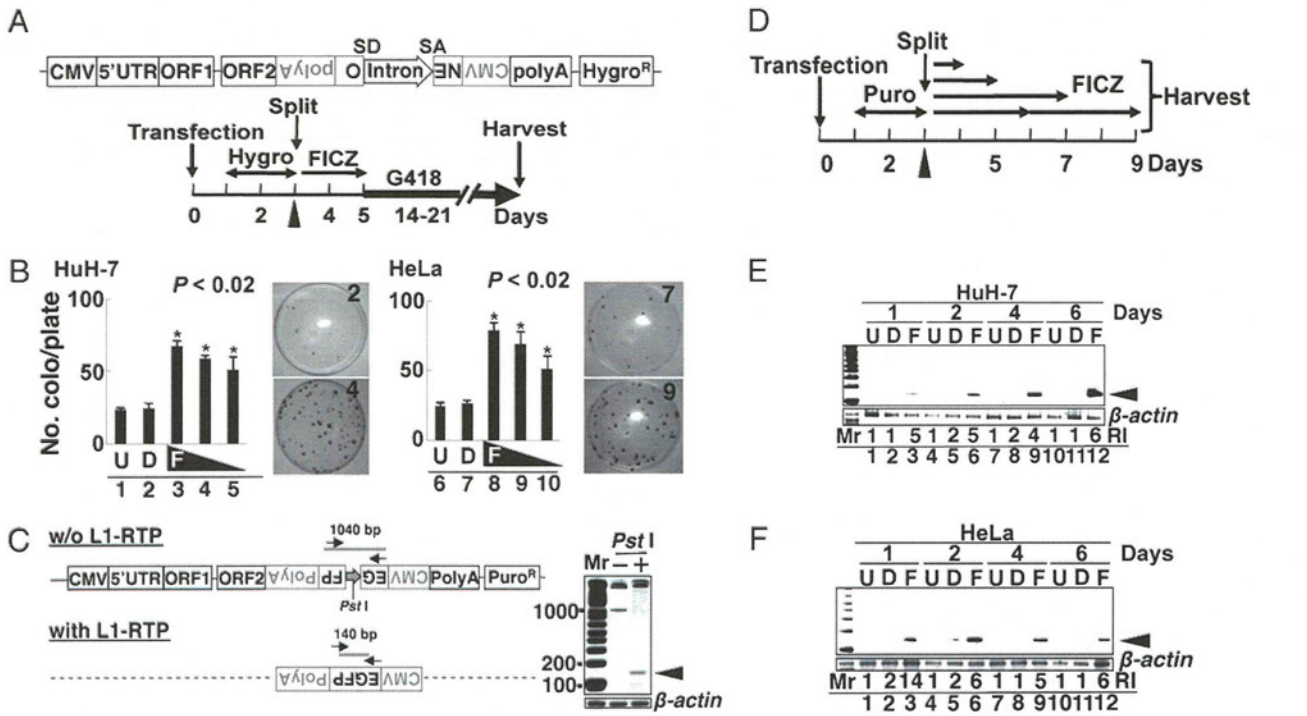

Fig. 1. FICZ induces L1-RTP. (*A*) Schematic diagram of pL1-Neo^R and the experimental protocol for the colony assay. Cells were transfected with pL1-Neo^R, selected for 2 d using Hygro, and exposed for 2 d to FICZ. Selection with G418 started on day 5. In some experiments, siRNAs of target genes were transfected on day 3 (arrowhead) followed by exposure to FICZ on the next day (*SI Methods*). (*B*) Colony assay results. Cells were treated with no reagents (U, lanes 1 and 6), 0.01% dimethyl sulfoxide (DMSO; D, lanes 2 and 7), or FICZ at 100, 10, and 1 nM (F, lanes 3–5 and 8–10). The numbers of colonies were normalized by viability (Fig. S1*A*). The mean numbers of colonies ± standard deviation (SD) are shown. Asterisks indicate statistical significance ($P < 0.02$). Stained plates are also shown. Plate numbers 2 and 4 are for HuH-7 cells and plate numbers 7 and 9 are for HeLa cells. The upper and lower plates revealed Neo^R colonies formed by 0.01% DMSO (2 and 7) or 10 nM FICZ (4 and 9), respectively. (*C*) Schematic diagram of pEF06R and the rationale for the PCR-based assay. pEF06R has a structure similar to that of pL1-Neo^R except for *EGFP* cDNA instead of the Neo^R gene. PCR primers targeting separate exons of *EGFP* cDNA (arrows) amplify a 1,040-bp or 140-bp fragment, depending on the induction of L1-RTP. The dotted line indicates the presence of similar structure of pEF06R. To selectively amplify the 140-bp band, DNA samples were treated with PstI (whose site is present in the intron) (*Right*, lane 2). (*D*) Experimental protocols for the PCR-based assays (*SI Methods*). After transfection of pEF06R, HuH-7 cells were cultured for 2 d in the presence of Puro. After exposure for 1–6 d to 10 nM FICZ, genomic DNAs were prepared and subjected to PCR-based analysis of L1-RTP. (*E* and *F*) Results of the PCR-based assays. Both HuH-7 (*E*) and HeLa (*F*) cells showed the amplified 140-bp band within 1 d after FICZ treatment (arrowheads). Relative intensities (RI) were calculated based on signal intensities of the 140-bp DNA and a DNA fragment of *β-actin* amplified as an internal control. D, 0.001% DMSO; F, 10 nM FICZ; U, untreated.

in Fig. 1*B*, L1-RTP was induced in both cell lines by FICZ at concentrations of 100, 10, and 1 nM (Fig. 1*B*, lanes 3–5 and 8–10; $P < 0.02$). No cytotoxic effects of the compound were detected even at 100 nM FICZ (Fig. S1*A*).

The induction of L1-RTP by FICZ was confirmed by a PCR-based assay with pEF06R (*SI Methods*) (7). As shown in Fig. 1*C*, PCR primers were designed in separate exons of *EGFP* cDNA, such that a 140-bp fragment would be amplified when L1-RTP was induced (Fig. 1*C*). By treating the sample DNAs with PstI (the site is present in the intron), the 140-bp band was selectively amplified (Fig. 1*C Right*, lane 2). According to the protocol shown in Fig. 1*D*, we carried out a time-course analysis of FICZ-induced L1-RTP. When 10 nM FICZ was applied, both HuH-7 cells and HeLa cells showed the 140-bp band within 1–2 d (Fig. 1 *E* and *F*). Additionally, the frequency of FICZ-induced L1-RTP was 10^{-4} to 10^{-5}, when estimated by the PCR-based assay (Fig. S1*B*).

FICZ-Induced L1-RTP Under Down-Regulation of Endogenous AhR. Because FICZ is an AhR ligand (14, 15), we examined whether AhR is required for FICZ-induced L1-RTP. As an initial experiment, we verified the effects of 3′-methoxy-4′-nitroflavone (MNF), an inhibitor of AhR (16). Notably, MNF did not reduce the FICZ-induced L1-RTP (Fig. S1*C*, lane 6), although it abolished the induction of *CYP1A1* mRNA (Fig. S1*D*, lane 6). Data strongly suggested that AhR is not required for the induction of L1-RTP by FICZ. To prove this, we carried out RNA-interference experiments using *AhR* siRNA. First, we confirmed that all three *AhR* siRNAs prepared, when used at 10 nM, could down-regulate the endogenous AhR to a level less than 20% that of the control (Fig. 2*A*; see also Fig. S2*A*). Then, we examined the effects of *AhR* siRNAs on the induction of L1-RTP by FICZ. Intriguingly, the induction of L1-RTP was observed even in the presence of these siRNAs (Fig. 2*B*; left and right panels depict the results with *AhR* siRNA-1 and -3, respectively). To gain further evidence, we carried out experiments under more stringent conditions. When 50 nM *AhR* siRNA was transfected into HuH-7 cells, the endogenous AhR was strongly suppressed for at least 3 d (Fig. 2*C*, lane 6). We next examined the effects of 2-d treatment of FICZ, and G418 selection was immediately started after FICZ exposure (Fig. 1*A*). Even under such conditions, FICZ induced L1-RTP (Fig. 2*D*, lane 6). Additionally, the activities of low doses of FICZ (1 and 0.1 nM) were examined under similar conditions (50 nM *AhR* siRNA) and again, the PCR-based assay detected L1-RTP (Fig. 2*E*, lanes 11 and 12). By transfecting 10 nM *AhR* siRNA, the induction of *CYP1A1* mRNA expression by FICZ was completely abolished (Fig. 2*F*, lane 9), indicating that endogenous AhR was functionally eliminated by the siRNA, although the residual amount of AhR was detectable.

Based on these data, we concluded that the induction of L1-RTP by FICZ is independent of AhR.

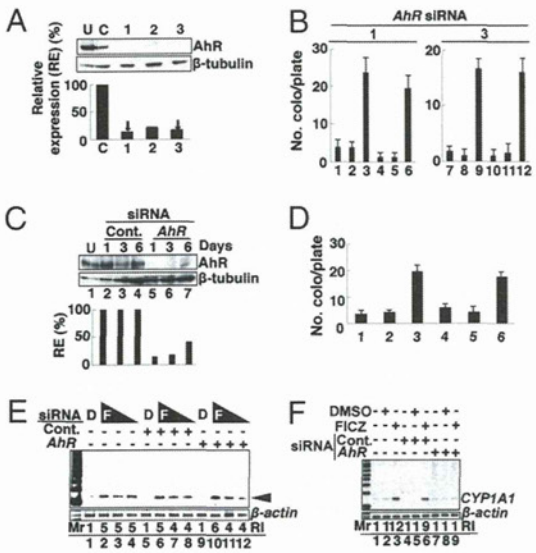

Fig. 2. AhR is dispensable for FICZ-induced L1-RTP. (*A*) Functional evaluation of *AhR* siRNAs. First, dose responses of *AhR* siRNAs for the suppression of endogenous AhR were verified (Fig. S2*A*). Then, the activities of three different *AhR* siRNAs (1–3) at 10 nM were examined. Relative expression (RE) of the AhR protein was calculated based on the expression levels of the proteins in the presence of control and *AhR* siRNAs. The RE was 11%, 19%, and 14% after transfection with *AhR* siRNA-1, -2, and -3, respectively. Arrows indicate the siRNAs used for the following experiments. (*B*) *AhR* siRNAs did not suppress FICZ-induced L1-RTP. Results of the colony assay performed in the presence of control siRNA (lanes 1–3 and 7–9) or *AhR* siRNAs (lanes 4–6 and 10–12 for siRNA-1 and -3, respectively) are shown. HuH-7 cells were treated with no reagents (lanes 1, 4, 7, and 10), 0.001% DMSO (lanes 2, 5, 8, and 11), or 10 nM FICZ (lanes 3, 6, 9, and 12). Mean numbers of colonies ± SD are shown. (*C*) Efficient suppression of endogenous AhR by siRNA. Western blot analysis was performed on days 1, 3, and 6 following the transfection of 50 nM *AhR* siRNA-1. The RE of AhR protein was calculated and plotted, indicating 13%, 16%, and 40% observed on day 1, 3, and 6 after transfection with *AhR* siRNA-1, respectively. Cont., control; U, untreated. (*D*) FICZ induced L1-RTP under stringent conditions. A colony assay was performed following the introduction of 50 nM control siRNA (lanes 1–3) or *AhR* siRNA-1 (lanes 4–6). HuH-7 cells were treated with no reagents (lanes 1 and 4), 0.001% DMSO (lanes 2 and 5), or 10 nM FICZ (lanes 3 and 6). G418 selection started immediately after FICZ treatment. Mean numbers of colonies ± SD are shown. (*E*) Low doses of FICZ induced L1-RTP under stringent conditions. On day 2 following the introduction of 50 nM control siRNA (lanes 5–8) or *AhR* siRNA-1 (lanes 9–12), HuH-7 cells were treated for 2 d with FICZ at 10 nM (lanes 2, 6, and 10), 1 nM (lanes 3, 7, and 11), or 0.1 nM (lanes 4, 8, and 12). Results of the PCR-based assay performed on the second day of FICZ treatment are shown. The arrowhead indicates L1-RTP. The RI of the 140-bp band was also calculated. (*F*) *AhR* siRNA suppressed *CYP1A1* mRNA expression. RT-PCR done on day 2 after introduction of 10 nM control siRNA (lanes 4–6) or *AhR* siRNA-1 (lanes 7–9) is shown. Cells were treated for 6 h with 10 nM FICZ and subjected to analysis. The RI was calculated based on the signal intensities of the transcript by the control and *AhR* siRNAs.

FICZ-Induced L1-RTP Is Dependent on ARNT1. Next, we examined the involvement of ARNT1 and observed that two different *ARNT1* siRNAs (1 and 2) efficiently suppressed the expression of endogenous ARNT1 (Fig. 3*A*; data with siRNA-1 and -2 are shown; see also Fig. S2*B*), and both siRNAs completely abolished FICZ-induced L1-RTP (Fig. 3*B*). The PCR-based assay also detected the inhibitory effects of the siRNA (Fig. S3*A*, lane 9), and the expression of *CYP1A1* mRNA was also inhibited by the siRNA (Fig. 3*C*, lane 9). Data suggested that the siRNA abrogated the function of endogenous ARNT1 and inhibited L1-RTP. To confirm this, we carried out a back-transfection experiment using siRNA-resistant *ARNT*1 cDNA (21). First, we confirmed that the introduction of a plasmid DNA expressing an siRNA-resistant *Flag-tagged ARNT1* mRNA (pSi^R-*ARNT1*; *SI Methods*) could restore the protein expression that had been reduced by the siRNA (Fig. 3*D*, lane 4). Then, we observed that pSi^R-*ARNT1* recovered the formation of Neo^R colonies, which had been suppressed by the siRNA (Fig. 3*E*, compare lanes 6 and 9; *SI Methods*). These data indicated that ARNT1 is involved in FICZ-induced L1-RTP.

To exclude the possibility that other cellular proteins related to the activity of AHRC are involved in FICZ-induced L1-RTP, we examined the effects of 10 nM siRNAs of *AhRR* (22) and *ARNT2* (23) on L1-RTP (Fig. S2 *C* and *D*). The results revealed that these molecules are not required for FICZ-induced L1-RTP (Fig. S3*B*, lanes 9 and 12).

Involvement of MAPK and CREB in the Induction of L1-RTP by FICZ. As TCDD activates MAPK (24), we tested the phosphorylation of MAPK substrates possibly related to the induction of L1-RTP. Among the three MAPK substrates examined, CREB was phosphorylated by FICZ (Fig. 4*A*, lane 3), whereas C/EBP-β and c-Jun were not (Fig. 4*A*). Notably, the FICZ-induced phosphorylation of CREB was abolished by the down-regulation of ARNT1 by siRNA (Fig. 4*B*, lane 6). We then examined the effects of MAPK inhibitors on FICZ-induced L1-RTP. As shown in Fig. 4*C*, the MAPK inhibitors, SB202190 for p38 (25) and SP600125 for JNK (26), efficiently suppressed L1-RTP (compare lanes 3, 6, and 7). The PCR-based assay revealed similar results, indicating the involvement of MAPK in FICZ-induced L1-RTP (Fig. S3*C*, lanes 6, 8, and 10).

To obtain direct evidence of the requirement of CREB for L1-RTP, the effects of *CREB* siRNAs were examined. Two different *CREB* siRNAs, which efficiently suppressed the expression of endogenous CREB protein (Fig. 3*D*, lanes 1 and 2), blocked L1-RTP (Fig. 4*E*; data with siRNA-1 and -2 are shown; see also Fig. S2*C*). Again, the PCR-based assay gave similar results (Fig. S3*D*, lane 9). Moreover, a plasmid DNA expressing an siRNA-resistant *Flag-tagged CREB* mRNA (pSi^R-*CREB*) successfully restored both CREB expression (Fig. 4*F*, lane 4) and L1-RTP (Fig. 4*G*, compare lanes 6 and 9). These data indicated that in response to FICZ, ARNT1 modulates the activity of MAPK, phosphorylates CREB, and induces L1-RTP.

Interestingly, SP600125 abrogated the induction of L1-RTP by FICZ, but we did not observe that FICZ induced the phosphorylation of c-Jun. Although SP600125 was originally proposed as a specific inhibitor of JNK (26), it was ascertained by subsequent studies that the compound could inhibit activities of several other protein kinases such as SGK, p70 ribosomal protein S6 kinase, AMPK, CDK2, and CK1δ (27). Data suggest the presence of an uncharacterized substrate(s), the activation of which is critical for L1-RTP by FICZ and sensitive to SP600125.

Chromatin Recruitment of ORF1 by FICZ-Dependent Activation of MAPK. Recently, Goodier et al. reported that ORF1, originally localized in cytoplasmic stress granules, is translocated to chromatin in response to stress stimuli (28). This led us to hypothesize that FICZ induces the nuclear trafficking of ORF1. To demonstrate this, we introduced a plasmid DNA encoding a chimeric protein composed of a codon-optimized ORF1 (29) tagged with a motif for tandem affinity purification (TAP) (30) into HuH-7 cells (*SI Methods*) and examined the FICZ-induced chromatin recruitment of ORF1. Western blot analysis revealed that FICZ increased ORF1 in the chromatin fraction (Fig. 5*B*, lane 2), although a slight amount of ORF1 was originally present in the chromatin fraction (Fig. 5*A*, lane 3). FICZ induced no increase in cellular ORF1 (Fig. S4 *A* and *B*) or ORF2 (Fig. S4 *C* and *D*). Immunoprecipitation followed by Western blot analysis revealed that FICZ triggered the complex formation of ORF1 and ARNT1 (Fig. 5*C*, compare lanes 4 and 8). Moreover, the MAPK inhibitor attenuated the FICZ-induced chromatin recruitment of ORF1 (Fig. 5*D*, compare lanes 3 and 6). Along with observations that the level of endogenous ARNT1 was not changed by FICZ (Fig. S4*E*),

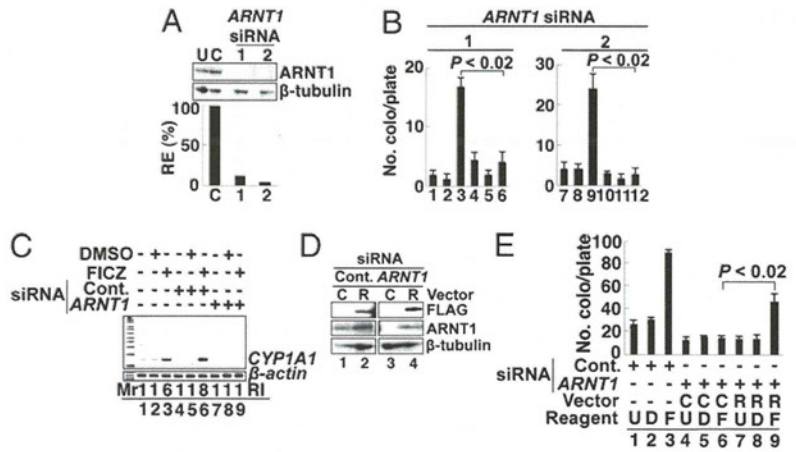

Fig. 3. ARNT1 is required for FICZ-induced L1-RTP. (*A*) Functional evaluation of *ARNT1* siRNAs. First, dose responses of *ARNT1* siRNAs for the suppression of endogenous ARNT1 were verified (Fig. S2*B*). Then, the activities of two different *ARNT1* siRNAs (1 and 2) at 10 nM were examined. The RE of endogenous ARNT1 protein was 12% and 4% when *ARNT1* siRNA-1 and -2 were introduced, respectively. (*B*) *ARNT1* siRNAs abrogated L1-RTP. A colony assay was performed on HuH-7 cells following the introduction of control siRNA (lanes 1–3 and 7–9) or *ARNT1* siRNA-1 and -2 (lanes 4–6 and 10–12). Cells were treated with no reagents (lanes 1, 4, 7, and 10), 0.001% DMSO (lanes 2, 5, 8, and 11), or 10 nM FICZ (lanes 3, 6, 9, and 12). Mean numbers of colonies ± SD are shown. The effects of *ARNT1* siRNAs were significant ($P < 0.02$). (*C*) Inhibitory effects of *ARNT1* siRNA on the expression of *CYP1A1* mRNA. Results of RT-PCR analysis with 10 nM control siRNA (lanes 4–6) or *ARNT* siRNA-1 (lanes 7–9) are shown. The RI of *ARNT1* mRNA is also given. (*D*) pSi^R-*ARNT1* restored protein expression. HuH-7 cells were introduced with control siRNA (lanes 1 and 2) or *ARNT1* siRNA-1 (lanes 3 and 4). On the next day, a control vector (C, lanes 1 and 3) or pSi^R-*ARNT1* (R, lanes 2 and 4) was transfected. Protein expression was detected by Western blot analysis on day 2 after the second transfection. (*E*) pSi^R-*ARNT1* recovered the L1-RTP suppressed by the siRNA. HuH-7 cells were transfected with *ARNT1* siRNA, followed by the introduction of a control vector (lanes 4–6) or pSi^R-*ARNT1* (lanes 7–9) on the following day. Then, cells were treated with 10 nM FICZ for 2 d followed by G418 selection. Mean numbers of colonies ± SD are shown. The difference between the number of Neo^R colonies obtained by pSi^R-*ARNT1* and by a control vector was significant ($P < 0.02$; compare lanes 6 and 9). C, control vector; D, 0.001% DMSO; F, 10 nM FICZ; R, pSi^R-*ARNT1*; U, untreated.

data indicated that FICZ mobilizes the L1 component to chromatin in a manner dependent on the activation of MAPK and ARNT1.

Discussion

In this study, we found that FICZ, a candidate physiological AhR ligand of a tryptophan photoproduct, induced L1-RTP. RNA-interference experiments conducted under strongly repressed expression of endogenous AhR suggested that AhR was not required for L1-RTP. In contrast, ARNT1, MAPK, and CREB were all involved in FICZ-induced L1-RTP. FICZ induced the association of ARNT1 and ORF1, and promoted the chromatin recruitment of ORF1 depending on the activation of MAPK. As the target of MAPK, CREB was pivotal for FICZ-induced L1-RTP, but our additional experiments revealed that the simple overexpression of a constitutively active form of *CREB* cDNA (p*CREB*^{Y134F}) (31) did not induce L1-RTP (Fig. S5). Additional functions of ARNT1 or MAPK are likely required for FICZ-induced L1-RTP.

We found that FICZ-induced L1-RTP was regulated in a fashion different from that induced by DNA double-strand breaks (DSB) (7). First, we observed that the time points of L1-RTP induced by FICZ and X-ray irradiation were different. In contrast, FICZ-induced L1-RTP was observed within 1–2 d (Fig. 1 *E* and *F*), but L1-RTP induced by DNA damage was observed only after 12 d of X-ray irradiation (Fig. S6*A*). Moreover, MAPK inhibitors

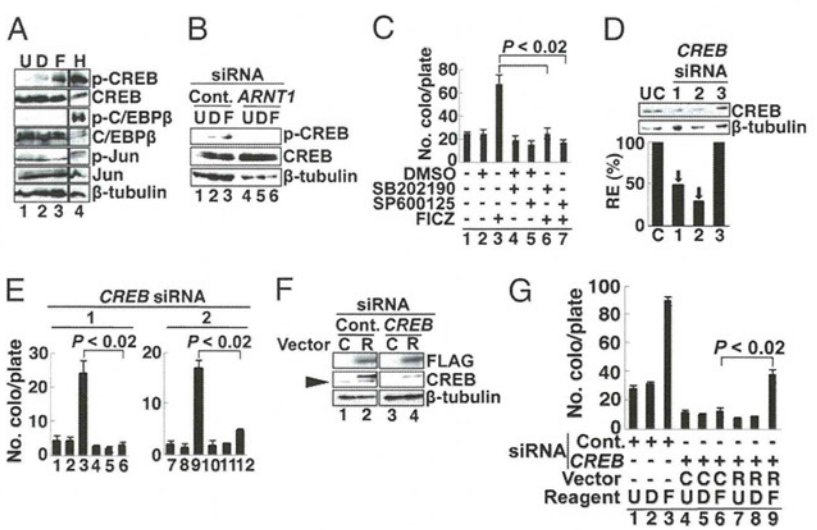

Fig. 4. MAPK and CREB are involved in L1-RTP. (*A*) Phosphorylation of CREB by FICZ. HuH-7 cells were treated with no reagents (U, lane 1), 0.001% DMSO (D, lane 2), 10 nM FICZ (F, lane 3), and 1 mM H_2O_2 (H, lane 4) as a positive control. Antibodies to nonphosphorylated or phosphorylated forms of CREB, C/EBP-β, and c-Jun were used. As a loading control, β-tubulin was detected. (*B*) FICZ-induced CREB phosphorylation depended on ARNT1. The FICZ-induced CREB phosphorylation was examined after introducing control siRNA (lanes 1–3) or *ARNT1* siRNA-1 (lanes 4–6). U, untreated (lanes 1 and 4); D, 0.001% DMSO (lanes 2 and 5); F, 10 nM FICZ (lanes 3 and 6). (*C*) Effects of MAPK inhibitors on L1-RTP. SB202190 (1 μM) and SP600125 (100 μM), which inhibit p38 and JNK, respectively, were added 30 min before the addition of 10 nM FICZ. Mean numbers of colonies ± SD are shown. The reductions in the numbers of Neo^R colonies by inhibitors were significant ($P < 0.02$; compare lanes 3, 6, and 7). (*D*) Functional evaluation of *CREB* siRNAs. First, dose responses of *CREB* siRNAs for the suppression of endogenous CREB were verified (Fig. S2*C*). Then, the activities of three different siRNAs (1–3) at 10 nM were examined. The RE of endogenous CREB protein was 48% and 28% when *CREB* siRNA-1 and -2 were introduced. *CREB* siRNA-3 was not effective. Arrows indicate the siRNAs used for the next experiments. (*E*) *CREB* siRNAs abrogated the L1-RTP. HuH-7 cells were transfected with 10 nM *CREB* siRNA-1 or -2, and treated with no reagents (lanes 1, 4, 7, and 10), 0.001% DMSO (lanes 2, 5, 8, and 11), or 10 nM FICZ (lanes 3, 6, 9, and 12). Then, a colony assay was carried out. Mean numbers of colonies ± SD are shown. *CREB* siRNA-1 (*Left*) and -2 (*Right*) significantly suppressed L1-RTP ($P < 0.02$). (*F*) pSi^R-*CREB* restored protein expression. HuH-7 cells were introduced with control siRNA (lanes 1 and 2) or *CREB* siRNA-1 (lanes 3 and 4) followed by transfection of a control vector (C) or pSi^R-*CREB* (R). CREB expression was checked on day 2 after transfection. Note that the band with a lower molecular weight is an endogenous CREB protein (lanes 1 and 2, arrowhead), which was abolished by *CREB* siRNA-1. (*G*) pSi^R-*CREB* recovered the L1-RTP suppressed by the siRNA. Experiments were performed as described (Fig. 3*E*). Mean numbers of colonies ± SD are shown. The difference between the number of Neo^R colonies recovered by pSi^R-*CREB* and a control vector was significant ($P < 0.02$; compare lanes 6 and 9). C, control vector; D, 0.001% DMSO; F, 10 nM FICZ; R, pSi^R-*CREB*; U, untreated.

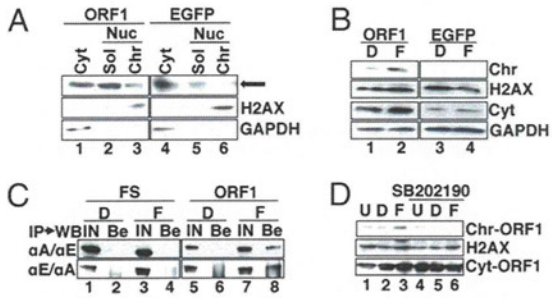

Fig. 5. The FICZ-induced chromatin recruitment of ORF1 depends on MAPK activity. (*A*) ORF1 present in the chromatin fraction. HuH-7 cells were transfected with plasmid DNAs encoding ORF1-TAP (lanes 1–3) or EGFP-TAP (lanes 4–6). On day 2 after transfection, cytoplasmic (Cyt, lanes 1 and 3), nuclear soluble (Sol, lanes 2 and 5), and chromatin (Chr, lanes 3 and 6) fractions were prepared and analyzed (*SI Methods*). H2AX and GAPDH were also detected to specify the subcellular localizations of the proteins. The arrow indicates the position of ORF1 in the chromatin fraction detected in lane 3. (*B*) Chromatin recruitment of ORF1 by FICZ. Similar experiments were done as described in *A*, and a chromatin fraction was prepared and analyzed 24 h after the addition of FICZ; 0.001% DMSO (D, lanes and 3); 10 nM FICZ (F, lanes 2 and 4). (*C*) FICZ stimulated the interaction of ARNT1 and ORF1. HuH-7 cells were transfected with p*FS-EGFP* (FS) (lanes 1–4) or p*ORF1-EGFP* (ORF1) (lanes 5–8). At 24 h after the addition of 0.001% DMSO (D, lanes 1, 2, 5, and 6) or 10 nM FICZ (F, lanes 3, 4, 7, and 8), cellular extracts were prepared and subjected to reciprocal experiments of immunoprecipitation (IP) followed by Western blot analysis (WB) (IP/WB). Upper row, IP with αARNT1 (αA) followed by WB using αE (αA/αE); lower row, IP with αEGFP (αE) followed by WB using αA (αE/αA). Both input sample (IN) (lanes 1, 3, 5, and 7) and protein recovered by protein G beads (Be) (lanes 2, 4, 6, and 8) were analyzed. As an IN sample, about one-tenth of the cell extract used for the IP was loaded. (*D*) MAPK inhibitor attenuated the chromatin recruitment of ORF1. SB202190 (1 μM) (lanes 4–6) was added 30 min before the addition of FICZ. U, untreated (lanes 1 and 4); D, 0.001% DMSO (lanes 2 and 5); F, 10 nM FICZ (lanes 3 and 6). ORF1 present in the chromatin fraction (Chr-ORF1 in top row) and cytoplasmic fraction (Cyt-ORF1 in bottom row) is shown. H2AX was also detected to specify the chromatin fraction (middle row). A similar result was obtained by an independent experiment.

completely blocked FICZ-induced L1-RTP (Fig. 4*C*), but not DSB-induced L1-RTP (Fig. S6*B*, lanes 7–9). Additionally, we found that TCDD was genotoxic, as judged by the increase of γ-H2AX (H2AX phosphorylated at serine 139), which is a sensitive cellular marker of DSB (32) (Fig. S6*C*, lanes 4 and 5), but it did not induce L1-RTP in HuH-7 cells (Fig. S6*D*), even though the same dose of TCDD induced the expression of CYP1A1 mRNA (Fig. S6*E*).

We carefully evaluated whether ARNT1 is a primary target involved in the rate-limiting process of FICZ-induced L1-RTP. Because XRE is present in the region of the 5′ UTR of human L1 (33) and mouse retroposons (34), we first excluded the possibility that FICZ induces L1-RTP by up-regulating the expression level of L1 mRNA. Quantitative RT-PCR analysis revealed that FICZ did not increase the expression of CMV-driven L1 mRNA (Fig. S7 *A* and *B*). Furthermore, MAPK inhibitors or siRNAs of *ARNT1* and *CREB* did not change the level of CMV-driven L1 mRNA (Fig. S7*B*, lanes 5–9). Additionally, FICZ did not increase the splicing efficiency of the immature L1 transcript (Fig. S7 *C* and *D*), *ORF2* mRNA (Fig. S7*E*), or the expression levels of ORF1/ORF2 proteins (Fig. S4 *B* and *D*). These findings strongly suggest that ARNT1 functions as the mediator for FICZ-induced L1-RTP.

ARNT1, as a central molecule of the class II bHLH/PAS proteins, either homodimerizes or promiscuously heterodimerizes with various bHLH/PAS members (9). As the best-characterized function, the NLS of ARNT1 contributes to nuclear trafficking of the ligand-bound AhR (11). Because ARNT1 has not been reported to function as a receptor to ligands, ARNT1 would likely associate with a novel molecule that binds FICZ. Interestingly, FICZ increases the mRNA expression of *Cry1* and *Cry2* genes, members of the bHLH/PAS family that are involved in the regulation of circadian rhythm (35). Furthermore, FICZ has been shown to change the electric activities of cells in the suprachiasmatic nucleus, where the master clock of circadian rhythm is maintained and controlled in response to light stimuli (36). These observations make it tempting to speculate that certain gene products involved in circadian rhythm can recognize FICZ, function as its receptor, and cooperate with ARNT1 for the induction of L1-RTP.

Our PCR-based assay revealed that picomolar levels of FICZ (3 pM) can induce L1-RTP (Fig. S8). About 8 pM FICZ was reported to be generated after a 24-h exposure of tissue-culture medium to ordinary laboratory light (14). Given that the concentration of tryptophan in human blood (about 70 μM) (37) is comparable to that present in tissue-culture medium (about 80 μM), FICZ may be generated in vivo and triggers L1-RTP. L1 is conserved in organisms from zebrafish to human (4), and a human L1 homolog of *Candida albicans* is competent for retrotransposition in *Saccharomyces cerevisiae* (38). Furthermore, cellular responses to FICZ have been reported in both a *Xenopus laevis* cell line (39) and zebrafish embryos (40), implying that FICZ can induce L1-RTP in various living organisms. Although further study is required, our current observations suggest the possibility that a member(s) of the bHLH/PAS family is involved in the epigenetic mode of L1-RTP. One possibility is that the genome shuffling by ARNT1-mediated L1-RTP provides living organisms the opportunity to acquire novel characteristics in response to environmental changes such as daylight.

Methods

Cells. HuH-7 cells (a human hepatocellular carcinoma cell line) and HeLa cells (a cervical carcinoma cell line) were used. The transfection efficiency of these cell lines, when judged by EGFP-positive cells after transfection of an *EGFP* expression vector, was about 70% and 30%, respectively.

L1-RTP Assays. Two different systems were used: a colony assay using pL1-Neo^R and a PCR-based assay using pEF06R. Each assay was performed at least twice, and representative results are presented. FICZ was used at 10 nM, unless stated otherwise.

RNA-Interference and Back-Transfection Experiments Using siRNA-Resistant Clones. Knockdown experiments were conducted using two different siRNAs for each gene. Each siRNA was used at 10 nM. To generate stringent conditions for down-regulated AhR expression, 50 nM *AhR* siRNA was used. Nucleotide sequences of used siRNAs were summarized in Table S1. The expression vectors for siRNA-resistant *ARNT1* and *CREB* cDNAs (pSi^R-*ARNT1* and pSi^R-*CREB*) and constitutively active CREB (p*CREB*^{Y134F}) were constructed based on pcDNA3.1 Zeo (+) (Invitrogen). Their quality was verified by restriction mapping and nucleotide sequencing.

Chromatin Recruitment of ORF1. Plasmid DNAs encoding *ORF1-TAP* (p*ORF1-TAP*) and *EGFP-TAP* (p*EGFP-TAP*) were generated using pcDNA3.1 Zeo. To prepare the DNA fragments, pBudORF1$_{syn}$ expressing a codon-optimized *ORF1* cDNA (29), pZome-1-C vector for *TAP-tag* cDNA (30), and pBOSH2BGFP-N1 for *EGFP* cDNA (41) were used.

Association of ORF1 and ARNT1. Plasmid DNAs encoding ORF1-EGFP (p*ORF1-EGFP*) and Flag-streptag EGFP (p*FS-EGFP*) were produced based on pcDNA3.1 Zeo. cDNA fragments were prepared from pBudORF1$_{syn}$ and pBOSH2BGFP-N1. p*FS-EGFP* was prepared by inserting an oligonucleotide cassette encoding -WSHPQFEK-WSHPQFEK-M- (amino acid sequence for 2xstreptag peptide is depicted by single letters, with spacers indicated by "-") into 5′ to *EGFP* cDNA that had been inserted in pFlag-CMV2 (Sigma).

Statistics. Statistical significance was evaluated using the Mann–Whitney *U* test. A *P* value of <0.05 was considered to be statistically significant.

Experimental procedures and construction of the plasmid DNAs are described in detail in *SI Methods*.

ACKNOWLEDGMENTS. We are grateful to Drs. Nicolas Gilbert (University of Michigan Medical School, Ann Arbor, MI), Eline T. Luning Prak (University of Pennsylvania School of Medicine, Philadelphia, PA), John Goodier (University of Pennsylvania School of Medicine, Philadelphia, PA), Gabriele Vielhaber (Symrise, Holzminden, Germany), Mark Hahn (Woods Hole Oceanographic Institution, Woods Hole, MA), Oliver Hankinson (Jonsson Comprehensive Cancer Center, University of California, Los Angeles, CA), Kumiko Saeki (National Center for Global Health and Medicine), Astrid M. Roy-Engel (Tulane University Health Sciences Center, New Orleans, LA), and Geoffrey M. Wahl (Salk Institute for Biological Studies, La Jolla, CA) for providing us with pCEP4/L1*mneoI*/ColE1, pEF06R, an antibody to ORF2, MNF, an antibody to AhRR, *ARNT1* cDNA, *CREB* cDNA, pBudORF1$_{syn}$/ORF2$_{syn}$, and pBOSH2BGFP-N1. Dr. Takuro Shimbo (National Center for Global Health and Medicine) kindly carried out statistical analysis of experimental data. This work was supported by a grant from the National Center for Global Health and Medicine (21A-104) and in part by a research grant for the Long-Range Research Initiative from the Japan Chemical Industry Association.

1. Bannert N, Kurth R (2004) Retroelements and the human genome: New perspectives on an old relation. *Proc Natl Acad Sci USA* 101 (Suppl 2):14572–14579.
2. Kazazian HH, Jr (2004) Mobile elements: Drivers of genome evolution. *Science* 303: 1626–1632.
3. Goodier JL, Kazazian HH, Jr (2008) Retrotransposons revisited: The restraint and rehabilitation of parasites. *Cell* 135:23–35.
4. Furano AV, Duvernell DD, Boissinot S (2004) L1 (LINE-1) retrotransposon diversity differs dramatically between mammals and fish. *Trends Genet* 20:9–14.
5. Brouha B, et al. (2003) Hot L1s account for the bulk of retrotransposition in the human population. *Proc Natl Acad Sci USA* 100:5280–5285.
6. Han JS, Szak ST, Boeke JD (2004) Transcriptional disruption by the L1 retrotransposon and implications for mammalian transcriptomes. *Nature* 429:268–274.
7. Farkash EA, Kao GD, Horman SR, Luning Prak ET (2006) Gamma radiation increases endonuclease-dependent L1 retrotransposition in a cultured cell assay. *Nucleic Acids Res* 34:1196–1204.
8. Hahn ME (2002) Aryl hydrocarbon receptors: Diversity and evolution. *Chem Biol Interact* 141:131–160.
9. Kewley RJ, Whitelaw ML, Chapman-Smith A (2004) The mammalian basic helix-loop-helix/PAS family of transcriptional regulators. *Int J Biochem Cell Biol* 36:189–204.
10. Denison MS, Nagy SR (2003) Activation of the aryl hydrocarbon receptor by structurally diverse exogenous and endogenous chemicals. *Annu Rev Pharmacol Toxicol* 43:309–334.
11. Eguchi H, Ikuta T, Tachibana T, Yoneda Y, Kawajiri K (1997) A nuclear localization signal of human aryl hydrocarbon receptor nuclear translocator/hypoxia-inducible factor 1β is a novel bipartite type recognized by the two components of nuclear pore-targeting complex. *J Biol Chem* 272:17640–17647.
12. Beischlag TV, Luis Morales J, Hollingshead BD, Perdew GH (2008) The aryl hydrocarbon receptor complex and the control of gene expression. *Crit Rev Eukaryot Gene Expr* 18:207–250.
13. Rannug A, et al. (1987) Certain photooxidized derivatives of tryptophan bind with very high affinity to the Ah receptor and are likely to be endogenous signal substances. *J Biol Chem* 262:15422–15427.
14. Oberg M, Bergander L, Håkansson H, Rannug U, Rannug A (2005) Identification of the tryptophan photoproduct 6-formylindolo[3,2-*b*]carbazole, in cell culture medium, as a factor that controls the background aryl hydrocarbon receptor activity. *Toxicol Sci* 85:935–943.
15. Wincent E, et al. (2009) The suggested physiologic aryl hydrocarbon receptor activator and cytochrome P4501 substrate 6-formylindolo[3,2-*b*]carbazole is present in humans. *J Biol Chem* 284:2690–2696.
16. Fritsche E, et al. (2007) Lightening up the UV response by identification of the arylhydrocarbon receptor as a cytoplasmatic target for ultraviolet B radiation. *Proc Natl Acad Sci USA* 104:8851–8856.
17. Quintana FJ, et al. (2008) Control of T(reg) and T(H)17 cell differentiation by the aryl hydrocarbon receptor. *Nature* 453:65–71.
18. Veldhoen M, et al. (2008) The aryl hydrocarbon receptor links TH17-cell-mediated autoimmunity to environmental toxins. *Nature* 453:106–109.
19. Saeki K, Saeki K, Yuo A (2003) Distinct involvement of cAMP-response element-dependent transcriptions in functional and morphological maturation during retinoid-mediated human myeloid differentiation. *J Leukoc Biol* 73:673–681.
20. Moran JV, et al. (1996) High frequency retrotransposition in cultured mammalian cells. *Cell* 87:917–927.
21. Hoffman EC, et al. (1991) Cloning of a factor required for activity of the Ah (dioxin) receptor. *Science* 252:954–958.
22. Baba T, et al. (2001) Structure and expression of the Ah receptor repressor gene. *J Biol Chem* 276:33101–33110.
23. Dougherty EJ, Pollenz RS (2008) Analysis of Ah receptor-ARNT and Ah receptor-ARNT2 complexes in vitro and in cell culture. *Toxicol Sci* 103:191–206.
24. Kwon M-J, Jeong K-S, Choi EJ, Lee BH (2003) 2,3,7,8-Tetrachlorodibenzo-*p*-dioxin (TCDD)-induced activation of mitogen-activated protein kinase signaling pathway in Jurkat T cells. *Pharmacol Toxicol* 93:186–190.
25. Lee HE, et al. (2009) Biphasic activation of p38MAPK suggests that apoptosis is a downstream event in pemphigus acantholysis. *J Biol Chem* 284:12524–12532.
26. Bennett BL, et al. (2001) SP600125, an anthrapyrazolone inhibitor of Jun N-terminal kinase. *Proc Natl Acad Sci USA* 98:13681–13686.
27. Bain J, McLauchlan H, Elliott M, Cohen P (2003) The specificities of protein kinase inhibitors: An update. *Biochem J* 371:199–204.
28. Goodier JL, Zhang L, Vetter MR, Kazazian HH, Jr (2007) LINE-1 ORF1 protein localizes in stress granules with other RNA-binding proteins, including components of RNA interference RNA-induced silencing complex. *Mol Cell Biol* 27:6469–6483.
29. Wallace N, Wagstaff BJ, Deininger PL, Roy-Engel AM (2008) LINE-1 ORF1 protein enhances Alu SINE retrotransposition. *Gene* 419:1–6.
30. Rigaut G, et al. (1999) A generic protein purification method for protein complex characterization and proteome exploration. *Nat Biotechnol* 17:1030–1032.
31. Du K, Asahara H, Jhala US, Wagner BL, Montminy M (2000) Characterization of a CREB gain-of-function mutant with constitutive transcriptional activity in vivo. *Mol Cell Biol* 20:4320–4327.
32. Rogakou EP, Pilch DR, Orr AH, Ivanova VS, Bonner WM (1998) DNA double-stranded breaks induce histone H2AX phosphorylation on serine 139. *J Biol Chem* 273: 5858–5868.
33. Stribinskis V, Ramos KS (2006) Activation of human long interspersed nuclear element 1 retrotransposition by benzo(a)pyrene, an ubiquitous environmental carcinogen. *Cancer Res* 66:2616–2620.
34. Roman AC, Benitez DA, Carvajal-Gonzalez JM, Fernandez-Salguero PM (2008) Genome-wide B1 retrotransposon binds the transcription factors dioxin receptor and Slug and regulates gene expression in vivo. *Proc Natl Acad Sci USA* 105:1632–1637.
35. Mukai M, Tischkau SA (2007) Effects of tryptophan photoproducts in the circadian timing system: Searching for a physiological role for aryl hydrocarbon receptor. *Toxicol Sci* 95:172–181.
36. Reppert SM, Weaver DR (2002) Coordination of circadian timing in mammals. *Nature* 418:935–941.
37. Suzuki Y, et al. (2010) Increased serum kynurenine/tryptophan ratio correlates with disease progression in lung cancer. *Lung Cancer* 67:361–365.
38. Dong C, Poulter RT, Han JS (2009) LINE-like retrotransposition in *Saccharomyces cerevisiae*. *Genetics* 181:301–311.
39. Laub LB, Jones BD, Powell WH (2010) Responsiveness of a *Xenopus laevis* cell line to the aryl hydrocarbon receptor ligands 6-formylindolo[3,2-*b*]carbazole (FICZ) and 2,3,7,8-tetrachlorodibenzo-*p*-dioxin (TCDD). *Chem Biol Interact* 183:202–211.
40. Jönsson ME, et al. (2009) The tryptophan photoproduct 6-formylindolo[3,2-*b*] carbazole (FICZ) binds multiple AHRs and induces multiple *CYP1* genes via AHR2 in zebrafish. *Chem Biol Interact* 181:447–454.
41. Kanda T, Sullivan KF, Wahl GM (1998) Histone-GFP fusion protein enables sensitive analysis of chromosome dynamics in living mammalian cells. *Curr Biol* 8:377–385.